

# The large-scale production of graphene flakes using magnetically-enhanced arc discharge between carbon electrodes

I. Levchenko <sup>a,b</sup>, O. Volotskova <sup>c</sup>, A. Shashurin <sup>c,d</sup>, Y. Raitses <sup>e</sup>, K. Ostrikov <sup>a,b</sup>, M. Keidar <sup>c</sup>

<sup>a</sup> CSIRO Materials Science and Engineering, P.O. Box 218, Lindfield NSW 2070, Australia

<sup>b</sup> School of Physics, The University of Sydney, Sydney NSW 2006, Australia

<sup>c</sup> Department of Mechanical and Aerospace Engineering, The George Washington University, Washington, DC 20052, USA

<sup>d</sup> Applied Plasma Science LLC, Marlowe Place, Oak Park, MI 25930, USA

<sup>e</sup> Princeton Plasma Physics Laboratory, Princeton, NJ 08543, USA

## ARTICLE INFO

### Article history:

Received 28 May 2010

Accepted 29 July 2010

Available online 7 August 2010

## ABSTRACT

A novel approach to large-scale production of high-quality graphene flakes in magnetically-enhanced arc discharges between carbon electrodes is reported. A non-uniform magnetic field is used to control the growth and deposition zones, where the Y-Ni catalyst experiences a transition to the ferromagnetic state, which in turn leads to the graphene deposition in a collection area. The quality of the produced material is characterized by the SEM, TEM, AFM, and Raman techniques. The proposed growth mechanism is supported by the nucleation and growth model.

© 2010 Elsevier Ltd. All rights reserved.

Graphene and graphene flakes (GFs) are very promising for various carbon-based nanodevices (single-electron transistors, supercapacitors, sensors, etc.) [1,2]. GFs also demonstrate unique mechanical properties, thus being the most prominent candidates for the micro- and nano-electromechanical systems [3]. With graphene's intrinsic breaking strength reaching  $42 \text{ N m}^{-1}$ , it is the strongest material ever discovered in the Universe. The production of graphene flakes usually requires very specific process conditions, namely a large influx of carbon material, relatively high temperatures, and often a specially prepared catalyst. These conditions can be easily maintained in high-density plasmas [4,5]. Recently, arc discharge plasmas have been successfully used for the synthesis of graphene flakes [6,7], but large-scale production of GFs still remains essentially unresolved. The majority of the surface-based methods (micro-mechanical exfoliation, epitaxial growth, decomposition of silicon carbide, etc.) have not reached the expected yields [1]. Thus, the arc discharge still remains the most promising method for synthesizing high-quality GFs at industrial scales. Given the phenomenal success of arc discharges in the synthesis of large amounts of high-quality CNTs, further development of the arc discharge systems for the effective large-scale production of graphene is a highly-topical issue.

Here we report on a novel method for the large-scale production of graphene flakes in an arc discharge, enhanced with a specially shaped magnetic field and a custom-designed catalyst. Using our approach, it is possible to achieve production yields of graphene flakes which exceed the rates achievable by other techniques.

The graphene flakes were produced in a high-current arc discharge setup (see scheme and photo in Fig. 1) with carbon anode and cathode installed in the non-magnetic vacuum chamber. The cathode is a rod of 12 mm dia., and the anode is a rod of 6 mm dia. with a hole in the centre of 3 mm dia. The hole was filled with a mixture of graphitic carbon and Y-Ni catalyst powders (in 1:4 ratio), with the average particle size of 0.04–4 mm. A discharge-enhancing permanent magnet ( $50 \times 50 \times 25 \text{ mm}$ ) was installed in the chamber to create a non-uniform magnetic field of 1.2 kG in the interelectrode gap of about 1 cm. The simulated topography of the magnetic field is shown in Fig. 1. The process was conducted in a helium gas at a pressure of 500 Torr, which is very effective for the carbon nanostructure production [8]; some more details can be found in our recent publications [9].

The production of graphene in the catalyst-free arc discharge process is also possible, but in this case the use of hydrogen-containing environment is required to terminate dangling bonds with hydrogen atoms and thus prevent the

\* Corresponding author at: CSIRO Materials Science and Engineering, P.O. Box 218, Lindfield NSW 2070, Australia. Fax: +61 2 9413 7634.

E-mail address: Kostya.Ostrikov@csiro.au (K. Ostrikov).

0008-6223/\$ - see front matter © 2010 Elsevier Ltd. All rights reserved.

doi:10.1016/j.carbon.2010.07.055

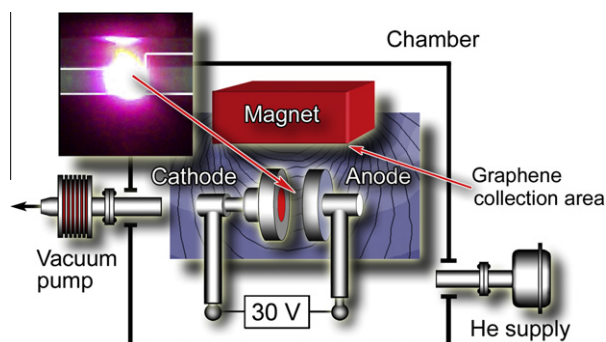


**Fig. 1** – Field emission scanning electron micrograph (FESEM) images (a) and (b), X-ray diffraction (XRD) pattern of carbon fibers annealed at 1400 °C for 2 h (c), transmission electron micrograph (TEM) image of carbon fibers with 5 wt.% cobalt (d, e) and SAED of cobalt particles (inset of figure e).

graphene sheets from rolling into nanotubes [7]. Since hydrogen exhibits high chemical activity in plasma (it can effectively reduce oxides and carbides), such process may lead to low controllability of graphene doping with some dopants. This is why we used a catalyzed process in a pure noble gas environment which is highly flexible with respect to any graphene compositions.

The application of an external magnetic field strongly increases both plasma density and temperature [8]. The plasma density is increased by the two main effects: first, by magnetic confinement that restricts the plasma, and second, by magnetizing electrons and thus creating conditions for more effective ionization of the neutral gas atoms [10]. Plasma temperature, in turn, increases the magnetic field due to stronger electric field in the magnetized plasma, in contrast to the non-magnetic conditions. This in turn results in the increase heating of the nanostructures in the plasma, and strongly increased flux of ionized material to the nanostructures; as a result, fast nucleation and growth is ensured due to the application of an external magnetic field.

The temperature of the anode surface reaches 3500 K [11], and thus, effective evaporation of the metal catalyst particles released from anode is ensured. In the discharge core, temperature reaches 5000 K and hence, further evaporation of the metal catalyst to the plasma is supported [12]. Then, the discharge temperature between electrodes falls down below 2000 K, and the metal catalyst re-nucleates and grows to small catalyst particles (4 nm in average). Further, when the temperature falls below 1500 K, nucleation and growth of the graphene flakes on the small newly-nucleated catalyst particles starts.

To optimize the growth and deposition of graphene flakes, we used the optimized composition of the two transition metals, Yttrium (paramagnetic, which easily forms carbides enabling a very quick nucleation of graphene) and Nickel (ferromagnetic with the Curie temperature of about 350 °C, a metal with very high carbon solubility which does not form carbon-containing compounds without oxygen and ensures an efficient carbon supply to the nanostructures). Thus, the catalyst nanoparticles remain non-magnetic in the hot zone

where a strong incoming flux of carbon material to the catalyst is maintained; outside of the growth zone, the gas temperature (and hence the catalyst temperature) decrease sharply below the Curie point. Consequently, the catalyst particles become ferromagnetic, respond to the magnetic field, and eventually the catalyst particles with the attached graphene flakes deposit on the magnet surface, in specific graphene collection areas. Thus, in our experiments the specially designed catalyst accelerated the nucleation and growth of graphene, and led to graphene deposition onto the magnet surface before any significant overgrowth takes place.

The carbon samples were analysed with SEM, TEM, AFM, and Micro-Raman techniques. The Micro-Raman system was based on an air-cooled argon 200 mW ion laser, holographic optics, spectrometer with a CCD detector (matrix size of 1100 × 330 pixels), power ~5 mW, wavelength 514 nm. A series of Raman measurements over both scattering ranges (first and second order, which allows to study second order peaks) were made. TEM (JEOL JEM-1200EX) and AFM (Asylum Research MFP3D, tapping-mode in air) imaging was used to investigate the structural properties of the graphene flakes. The AFM tip (Olympus AC240TS silicon cantilevers, force constant  $k = 2 \text{ N m}^{-1}$ , resonance frequency  $f = 70 \text{ kHz}$ ) was used in the analysis. The high-resolution SEM analysis was performed using a Hitachi field emission S-4700-II FE-SEM microscope (accelerating voltages from 1 to 30 kV). The samples for TEM analysis were prepared by dispersion of the carbon soot into aqueous 2% (mass/volume) sodium deoxycholate solution by sonicating in ice bath for 1 h at 1 W/mL of the applied power. Then, the sonicated suspension was centrifuged in a Beckman J-2 centrifuge for 2 h in a JA-20 rotor at a speed of 1885 rad/s and a temperature of 10 °C. After that, the samples were placed on a gilder grid (T2000-Cu, square, Electron Microscopy Science) for further microanalysis.

In Fig. 2 we show SEM micrographs of carbon material collected on the magnet surfaces, TEM image and SAED pattern of graphene flakes. The estimated size of the GFs is approximately 500–2500 nm, typically with up to 10 graphene layers. The atomic force microscopy clearly revealed the presence of flake-like structures with the size of around one micron and a fairly uniform height in the 1–5 nm range (Fig. 2e–g). This corresponds to 3–15 graphene layers in different areas of the flakes. The Raman characterization of the specimens showed the occurrence of a weak D-peak at around  $1325 \text{ cm}^{-1}$ , which is related to the relatively small amount of defects in  $sp^2$  bonds (Fig. 2h). G-peak at  $\approx 1582 \text{ cm}^{-1}$  and highly symmetrical 2D-peak at  $\approx 2650 \text{ cm}^{-1}$  demonstrate the presence of a relatively small number of graphene layers in the flakes. It should be noted that carbon nanotubes were also found in samples collected elsewhere in the chamber.

The absolute maximum of the graphene flake production yield in the arc discharge with carbon electrodes can be estimated using the measured ablation rate of the graphite anode. In our experiment, the ablation rate is about  $3 \text{ g} \times \text{min}^{-1}$  [13]. The production yield of the multilayered graphene flakes in our experimental setup is about  $0.3 \text{ g} \times \text{h}^{-1} \times \text{m}^{-2}$  for the discharge current 50 A. Moreover, the production rate can be scaled up by increasing the arc current. Our previous studies suggest that the carbon supply rate increases linearly with arc current [11]; thus, the graphene

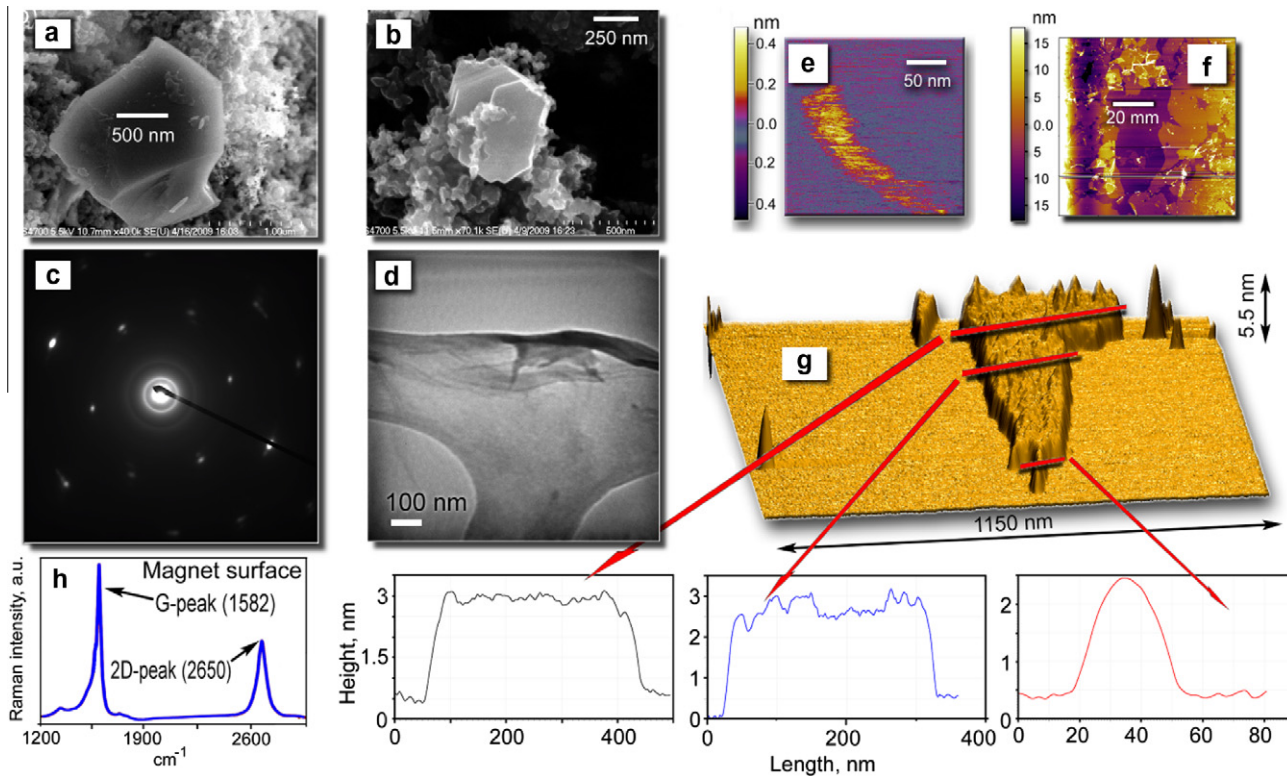


**Fig. 2** – SEM, TEM, AFM, and Raman characterization of the pristine (a and b) and processed (c–g) samples collected from the magnet surfaces. Representative SEM images of the carbon nanoparticles containing graphene flakes (a and b); SAED pattern of the carbon material (c); TEM image of the folding graphene layers (d); 2D (e and f) and 3D (g) AFM images of two graphene flake samples. Three profiles of the AFM image illustrate the flake structure containing several graphene layers (total thickness 2–3 nm); Representative Raman spectra of the graphene flake samples (h). G-peak at  $\approx 1582 \text{ cm}^{-1}$  and symmetrical 2D-peak at  $\approx 2650 \text{ cm}^{-1}$  demonstrate the presence of a relatively small number of graphene layers in the flakes.

production can be scaled up to  $\approx 1 \text{ g} \times \text{h}^{-1} \times \text{m}^{-2}$  by increasing the arc current to 100–150 A. These numbers are significantly superior to the existing methods [14].

Let us now examine the growth mechanism of graphene flakes in the plasma of magnetic field-enhanced arc, focusing on the conditions that ensure formation of large single layer graphene fragment (SLGF), the most preferred form of the 2D carbon. We assume here the following growth scenario for the formation of a large multi-layered flake in the plasma. First, an SLGF (base layer) nucleates, and then it grows to a larger radius, without formation of additional layers on the top of the SLGF. Later, when the SLGF reaches a critical size, a new graphene layer nucleates on the top of SLGF; thus, a two-layer graphene flake is formed. Further, both SLGF (base layer) and newly-nucleated second graphene layer grow and after some time a new (third) graphene layer is formed, turning the two-layer flake into a three-layer graphene flake. The process continues till the flake is deposited in the collection area. It is clear that the first-nucleated (base) graphene layer is the largest and as such, it determines the size (radius) of the whole flake.

It is apparent that the main prerequisite for the formation of a large SLGF is the low density of carbon atoms adsorbed on a single (base) graphene layer. The SLGF is small at the first stage of the growth, and an atom deposited on the SLGF

leaves the surface before another atom deposits onto the SLGF. In this case, no nucleation of a new layer is possible on the base layer, and the SLGF grows as a single-layer fragment (most preferred form). When the carbon influx to the SLGF (base layer) exceeds the carbon outflux, conditions for the carbon adatom accumulation on the SLGF are satisfied, and hence, the new graphene layer nucleates, turning the SLGF into a two-layer flake. To estimate the critical SLGF size,  $R_c$ , we consider the four main processes of the SLGF growth, namely, the carbon influx to the SLGF surface, outflux from the surface by surface diffusion to the graphene edges followed by attachment to the edges and thus incorporating into the graphene structure, evaporation from the graphene surface, and removal of the carbon adatoms by direct impact of the gas molecules [15].

Carbon flux to the SLGF surface can be estimated as  $v_{\text{dep}} = V_i n_p S$ ,  $s^{-1}$ , where  $n_p$  is the carbon ion density,  $V_i$  is the ion velocity, and  $S$  is the SLGF surface area. Assuming the Bohm velocity  $V_B = (kT_e/m_i)^{1/2}$ , where  $k$  is the Boltzmann's coefficient,  $T_e$  is the electron temperature, and  $m_i$  is the carbon ion mass, we obtain  $v_{\text{dep}} = \pi R^2 n_p \sqrt{kT_e/m_i}$ . The carbon adatom outflux from the surface by surface diffusion to the edges can be estimated using the relation for a random walk distance  $R^2 = D_s t$ , where  $D_s$  is the surface diffusion coefficient, and  $t$  is the characteristic diffusion time. Since  $4D_s = \lambda^2 v_0 \times$

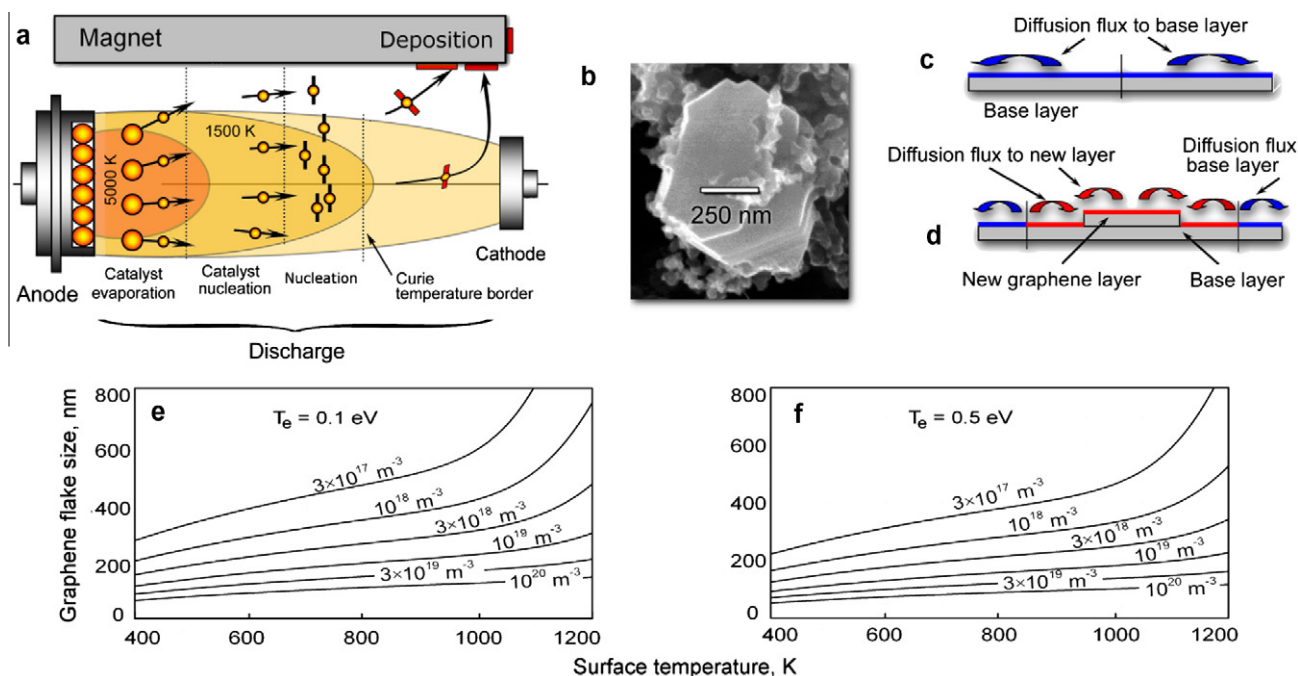


**Fig. 3 – Scheme of graphene nucleation, growth, and deposition in the magnetic field-enhanced arc discharge. Catalyst particles evaporate in a hot (5000 K) plasma, then nucleate into small (4 nm in average) particles at a lower temperature; further, graphene nucleation starts (a). Electron micrograph of a typical carbon nanoparticle containing graphene flakes (b); schematic of the single-layer growth (c) and nucleation of the second graphene layer (d). A strong carbon influx leads to faster formation of the new layers compared to the spreading of the existing layers; the resulting graphene fragment consists of several layers of approximately the same size (d); Dependence of the minimum graphene fragment size on the surface temperature, with the plasma density and the electron temperature ( $T_e$ ) as parameters (e and f).**

$\exp(-\epsilon_d/kT_s)$ , where  $v_0 = 2kT_S/h$  is the lattice oscillation frequency,  $h$  is the Planck's constant, and  $\epsilon_d$  is the surface diffusion activation energy, we obtain  $v_{\text{esc}} = [\lambda^2 kT_S/R^2 2h] \times \exp(-\epsilon_d/2kT_S)$ . The frequency of carbon adatom evaporation from the surface is:  $v_e = v_0 \times \exp(-\epsilon_a/kT_s)$ , or finally,  $v_e = [2kT_S/h] \times \exp(-\epsilon_a/kT_s)$ , where  $T_s$  is the graphene temperature and  $\epsilon_a$  is the evaporation energy. The frequency of the carbon adatoms removal by direct impact of the gas molecules can be estimated as a total frequency of adatom collisions with gas molecules that have an energy exceeding the C adatom evaporation energy, i.e.,  $v_c = V_c n_g \lambda^2 \times \exp(-\epsilon_a/kT_g)$ , where  $V_c = (2kT_g/m_c)^{1/2}$  is the gas atom velocity,  $n_g = P_g/(kT_g)$ ,  $P_g$  and  $T_g$  are the gas density, pressure, and temperature. Finally, we obtain:  $v_c = \lambda^2 P_g \sqrt{2/m_c kT_g} \times \exp(-\epsilon_a/kT_s)$ .

The critical SLGF radius is determined by the balance between the four fluxes, i.e.  $v_{\text{dep}} = v_{\text{esc}} + v_e + v_c$ . As it follows from the above model, the graphene surface temperature, as well as the plasma density and electron temperature are the most important parameters which determine the size of a single layer graphene fragment; thus, we made calculations for the typical arc plasma density range ( $10^{18} \dots 10^{20} \text{ m}^{-3}$ ) and two typical electron temperatures (0.1 and 0.5 eV), for the surface temperature range 400–1200 K. The calculated dependencies of the minimum graphene fragment size on the surface temperature, with the plasma density and the electron temperature as parameters, are

shown in Fig. 3e and f. Comparing these graphs with the graphene size shown in SEM image, one can see that the above model predicts reasonably well the GF size observed in the arc discharge.

Our unique, yet simple and environmentally-benign plasma-enabled approach demonstrates a novel technique for the effective large-scale synthesis of the high-quality graphene flakes in arc discharge plasmas. This in turn offers tantalizing prospects for the numerous applications in molecular sensors, single-electron transistors, supercapacitors, non-volatile memory devices, integrated circuits, atomic-scale switches and other carbon-based electronic and magneto-electronic devices.

## Acknowledgement

This work was supported in part by NSF/DOE Partnership in Plasma Science and Technology (NSF Grant CBET-0853777, DOE Grant DE-SC0001169), NSF STTR program, Grant IIP-1010133 (USA), and CSIRO's OCE Science Leadership Program (Australia). We would like to acknowledge PPPL Offsite Research Program supported by Office of Fusion Energy Sciences (USA) for supporting arc discharge experiments. Authors thank Jon Torrey for help with AFM. Fruitful discussions with S. Kumar are gratefully acknowledged.

## REFERENCES

- [1] Novoselov KS, Jiang D, Schedin F, Booth TJ, Khotkevich VV, Morozov SV, et al. Two-dimensional atomic crystals. *Proc Natl Acad Sci USA* 2005;102:10451–3.
- [2] Kyotani T, Ma Z, Tomita A. Template synthesis of novel porous carbons using various types of zeolites. *Carbon* 2003;41:1451–9.
- [3] Westervelt RM. Graphene nanoelectronics. *Science* 2008;320:324–5.
- [4] Tsakadze Z, Levchenko I, Ostrikov K, Xu S. Plasma-assisted self-organized growth of uniform carbon nanocone arrays. *Carbon* 2007;45:2022–30.
- [5] Cvelbar U, Chen Z, Sunkara MK, Mozetic M. Spontaneous growth of superstructure-Fe<sup>203</sup> nanowire and nanobelt arrays in reactive oxygen plasma. *Small* 2008;4:1610–4.
- [6] Karmakar S, Kulkarni NV, Nawale AB, Lsalla NP, Mishra R, Sathe VG, et al. *J Phys D Appl Phys* 2009;42:115201.
- [7] Subrahmanyam KS, Panchakarla LS, Govindaraj A, Rao CNR. Simple method of preparing graphene flakes by an arc-discharge method. *J Phys Chem C* 2009;11:4257–9.
- [8] Keidar M, Waas AM, Raites Y, Waldorff E. Modeling of the anodic arc discharge and conditions for single-wall carbon nanotube growth. *J Nanosci Nanotechnol* 2006;6:1309–15.
- [9] Keidar M, Levchenko I, Arbel T, Alexander M, Waas AM, Ostrikov K. Magnetic-field-enhanced synthesis of single-wall carbon nanotubes in arc discharge. *J Appl Phys* 2008;103:094318.
- [10] Keidar M, Levchenko I, Arbel T, Alexander M, Waas AM, Ostrikov K. Increasing the length of single-wall carbon nanotubes in a magnetically enhanced arc discharge. *Appl Phys Lett* 2008;92:043129.
- [11] Keidar M, Belis I. Modeling of atmospheric-pressure anodic carbon arc producing carbon nanotubes. *J Appl Phys* 2009;106:103304.
- [12] Volotskova O, Shashurin A, Keidar M, Raites Y, Demidov V, Adams S. Ignition and temperature behavior of a single-wall carbon nanotube sample. *Nanotechnol* 2010;21:095705.
- [13] Shashurin A, Keidar M, Beilis II. Voltage–current characteristics of an anodic arc producing carbon nanotubes. *J Appl Phys* 2008;104:063311.
- [14] Segal M. Selling graphene by the ton. *Nature Nanotech* 2009;4:612–4.
- [15] Levchenko I, Ostrikov K, Mariotti D. The production of self-organized carbon connections between Ag nanoparticles using atmospheric microplasma synthesis. *Carbon* 2008;47:344–7.

## Tubular carbon nanostructures produced by tunneling of cobalt nanoparticles in carbon fibers

Jianlin Li <sup>a</sup>, Xi Yi <sup>a</sup>, Haitao Ye <sup>b</sup>

<sup>a</sup> School of Materials Science and Engineering, Shanghai University, 149 Yanchang Road, Shanghai 200044, China

<sup>b</sup> School of Engineering and Applied Science, Aston University, Birmingham B4 7ET, UK

## ARTICLE INFO

## Article history:

Received 9 June 2010

Accepted 13 August 2010

Available online 20 August 2010

## ABSTRACT

Tubular carbon nanostructures have been produced by the tunneling of cobalt nanoparticles in carbon fibers that are derived from electrospun polyacrylonitrile (PAN) fibers. During the annealing in a vacuum up to 1400 °C, carbonization takes place to the cobalt-doped PAN fibers, causing these fibers to transform to a composite of cobalt nanoparticles and carbon fibers. Cobalt nanoparticles embedded in the carbon fibers start tunneling in these fibers, thus producing various tubular carbon nanostructures. During the tunneling, carbon atoms confronted with the cobalt nanoparticles diffuse into these particles, which later precipitate from them and leave a tubular structure behind.

© 2010 Elsevier Ltd. All rights reserved.

Since the landmark paper on carbon nanotubes (CNTs) by Iijima [1], tremendous efforts have been devoted to the study of these nanometer-sized tubes for anticipated, potential applications [2]. A variety of methods have been used to fabricate CNTs, amongst which two general strategies are em-

ployed. One strategy is to assemble carbon atoms into tubes, as reported by Chen et al. [3]. The other is to get graphene layers to roll-up into tubes [4].

When used as electronic components, which lie in one of the most important potential application fields of CNTs,

Corresponding author: Fax: +86 21 56331429.

E-mail addresses: jlli@shu.edu.cn, l\_j\_li@yahoo.com (J. Li).

0008-6223/\$ - see front matter © 2010 Elsevier Ltd. All rights reserved.

doi:10.1016/j.carbon.2010.08.037